Detection of GW bursts with chirplet-like template families

Éric Chassande-Mottin, Miriam Miele, Satya Mohapatra, Laura Cadonati

Detection of GW bursts with chirplet-like template families

Éric Chassande-Mottin[⋆], Miriam Miele[⋆†], Satya Mohapatra[‡] and Laura Cadonati[‡]

[⋆] CNRS and Univ. Paris Denis Diderot, AstroParticule et Cosmologie (France)
[†] ERASMUS fellow from the University of Sannio at Benevento (Italy)
[‡] Physics Department, University of Massachusetts, Amherst MA 01003 (USA)

E-mail: ecm@apc.univ-paris7.fr

Abstract. Gravitational Wave (GW) burst detection algorithms typically rely on the hypothesis that the burst signal is "locally stationary", that is it changes slowly with frequency. Under this assumption, the signal can be decomposed into a small number of wavelets with constant frequency. This justifies the use of a family of sine-Gaussian wavelets in the Omega pipeline, one of the algorithms used in LIGO-Virgo burst searches. However there are plausible scenarios where the burst frequency evolves rapidly, such as in the merger phase of a binary black hole and/or neutron star coalescence. In those cases, the local stationarity of sine-Gaussians induces performance losses, due to the mismatch between the template and the actual signal. We propose an extension of the Omega pipeline based on chirplet-like templates. Chirplets incorporate an additional parameter, the *chirp rate*, to control the frequency variation. In this paper, we show that the Omega pipeline can easily be extended to include a chirplet template bank. We illustrate the method on a simulated data set, with a family of phenomenological binary black-hole coalescence waveforms embedded into Gaussian LIGO/Virgo–like noise. Chirplet-like templates result in an enhancement of the measured signal-to-noise ratio.

1. Motivations

Current searches for gravitational wave transients in LIGO-Virgo data focus on two signal classes: short unmodelled bursts and longer quasi-periodic signals from inspiralling black hole and/or neutron star binaries as predicted by post-Newtonian approximations. To account for intermediate scenarios, we consider "chirping burst" GW target signals that exhibit characteristics from both the above categories: a short duration and a "sweeping" frequency.

We propose here an extension of the Omega pipeline [3] (originally known as $Q-$pipeline) that searches for chirping bursts. The Omega pipeline projects the data over a family of sine-Gaussian wavelets with fixed frequency. The idea is to replace these templates by frequency varying waveforms, referred to as *chirplets*.

In this paper, we first define chirplets and the related *chirplet transform*. We discuss the implementation of the chirplet transform and its insertion into the Omega pipeline, with attention to how the chirplet template bank is built. Finally, we present a few examples using simulated data.

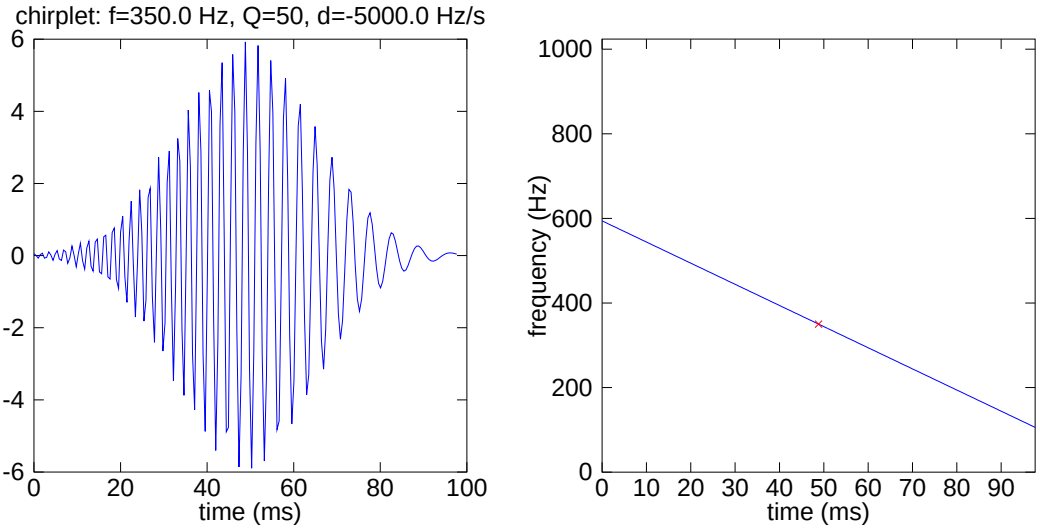

Figure 1. Example of a chirplet

2. From wavelets to chirplets

2.1. Definition of chirplets

Chirplets are defined in the time domain as:

$$\psi(\tau) \equiv A \exp\left(-\frac{(2\pi f)^2}{Q^2}(\tau - t)^2\right) \exp\left(2\pi i \left[f(\tau - t) + d/2\,(\tau - t)^2\right]\right), \tag{1}$$

with $A = (8\pi f^2/Q^2)^{1/4}$, a normalization factor ensuring that $\int |\psi|^2 = 1$. t and f are the center time and frequency, respectively and Q is the dimensionless quality factor. See in Fig. 1 for an example of a chirplet.

The main difference from a sine-Gaussian wavelets is the *chirp rate*, an additional term in the phase denoted d that changes the chirplet frequency linearly in time as $f(\tau) = f + d(\tau - t)$. The chirp rate controls the slope of the frequency evolution. When $d = 0$, we retrieve standard sine-Gaussians. Chirplets are thus associated with a four-dimensional parameter space instead of three for sine-Gaussians. In the sequel, we will concatenate all those parameters into a descriptor $\boldsymbol{\theta} \equiv \{t, f, Q, d\}$.

2.2. Chirplet transform

The *chirplet transform* T is obtained by correlating the data with the chirplets defined in the previous section. In the frequency domain, it reads:

$$T[x; \boldsymbol{\theta}] = \left| \int X(\xi) \Psi^*(\xi; \boldsymbol{\theta}) d\xi \right|^2, \tag{2}$$

where $X(\cdot)$ and $\Psi(\cdot; \boldsymbol{\theta})$ denotes the Fourier transform of the (whitened) data stream $x(\cdot)$ and chirplet $\psi(\cdot)$ with descriptor $\boldsymbol{\theta}$ resp.

The chirplet Fourier transform can be expressed as

$$\Psi(\xi; \boldsymbol{\theta}) = \mathcal{A} \exp\left(-\frac{\tilde{Q}^2}{4}\frac{(\xi - f)^2}{f^2}\right), \tag{3}$$

where $\mathcal{A} = [(\tilde{Q}^4/Q^2)/(2\pi f^2)]^{1/4}$ is written in terms of a "complex-valued" quality factor $\tilde{Q} = Q\sqrt{z}/|z|$ where $z = 1 + id\Delta_t^2$ with the chirplet duration[1] $\Delta_t = Q/(2\sqrt{\pi}f)$.

3. Building template banks with chirplets

By varying the chirplet parameters, we obtain a continuous signal space. In this space, we need to select a finite-size family of representatives which will be used to analyze the data. The coverage of the chirplet space has to meet two conflicting goals i.e., satisfy a worst case mismatch with a minimum number of templates. We adopt the method proposed in [4, 3] which consists of sampling the space with equi-spaced templates using the intrinsic *metric* deduced from the *mismatch* $T\left[\psi(\boldsymbol{\theta}');\boldsymbol{\theta}\right]$ between two neighboring templates with a small discrepancy $\delta\boldsymbol{\theta} \equiv \boldsymbol{\theta}' - \boldsymbol{\theta}$ in their parameters. The metric results from the second-order expansion of the mismatch $\mu_{\boldsymbol{\theta}}(\delta\boldsymbol{\theta}) \equiv 1 - T\left[\psi(\boldsymbol{\theta} + \delta\boldsymbol{\theta});\boldsymbol{\theta}\right] \approx \delta s^2$ when $\delta\boldsymbol{\theta} \to \mathbf{0}$ and leads to[2]:

$$\delta s^2 = \frac{Q^4 d^2 + 16\pi^2 f^4}{4Q^2 f^2}\delta t^2 + \frac{2+Q^2}{4f^2}\delta f^2 + \frac{\delta Q^2}{2Q^2} + \frac{Q^4}{128\pi^2 f^4}\delta d^2 - \frac{Q^2 d}{2f^2}\delta t\delta f - \frac{\delta f \delta Q}{Qf}. \qquad (4)$$

There are several differences and additional terms from the sine-Gaussian metric, due to the non-zero chirping rate. Along the time axis and for small $f \lesssim Q\sqrt{d}$, the sampling step $\delta t \propto f/(Qd)$ is finer than that of the sine-Gaussian case $\delta t \propto Q/f$. We note also that the sampling step along the chirping rate axis scales with $\delta d \propto (f/Q)^2$. We thus expect to get many chirplets in the low-frequency band and for large values of Q.

The chirplet space equipped with the above metric (off-diagonal terms being neglected for simplicity [3]) can be discretized by a cubic lattice with templates placed at the vertices. The worst case occurs when the real signal is farther apart from all vertices, at the center of the cube. Let us denote $\delta s = \mu^{1/2}$, this worst-case distance, which corresponds to the half-length of the cube diagonal and assign a maximum value $\mu_{\max}^{1/2}$ that we can tolerate. Since we are in a four-dimensional space, the length ℓ of the cube edge is equal to that of its half-diagonal. Therefore, we must have $\ell \leq \sqrt{\mu_{\max}}$. The discretization along each axis of the parameter space which results directly from this condition ensures that $\mu_{\boldsymbol{\theta}}(\boldsymbol{\theta} - \boldsymbol{\theta}_n) \leq \mu_{\max}$ for any $\boldsymbol{\theta}$ with $\boldsymbol{\theta}_n$ the closest vertex of the lattice. In the following, we set the maximum mismatch to the value $\mu_{\max} = 0.2$ typically used when applying standard Omega. Fig. 2 shows an example of a chirplet template bank resulting from this template placement scheme.

In Fig. 3, we apply the same scheme in two different settings. In both cases we computed the number of templates necessary to cover the signal space in the sine-Gaussian (standard Omega) and chirplet (chirpletized Omega) cases. This computation is done at a fixed time t. We compare the result to the estimate given by the ratio of the whole space volume $V = \int |\boldsymbol{\mu}^\star|^{1/2} d^3\boldsymbol{\theta}^\star$ (where $\boldsymbol{\theta}^\star = \{f, Q, d\}$ and $\delta s^2 = |\boldsymbol{\mu}^\star|$ denotes the metric in Eq. (4) without the components associated to the time axis) to the size of a cubic element of the lattice. We find[3]:

$$\mathcal{N} \equiv V/\ell^3 \propto f_{\min}^{-2} Q_{\max}^3 d_{\max}, \qquad (5)$$

where we assume that for each coordinate the lower boundaries (min) are much smaller than the higher boundaries (max).

It is important to note that both the count and estimate are obtained assuming an infinite bandwidth. Since the data are sampled, we are restricted to a limited Nyquist frequency.

[1] By definition, $\Delta_t \equiv 2\sqrt{\pi}\int(\tau - t)^2\psi^2(\tau)d\tau$.

[2] This calculation assumes that the detector noise has a flat spectrum. Contrarily to the sine-Gaussian case, this approximation has significant effect since the chirplet frequency varies across the detector bandwidth.

[3] This result is valid both when neglecting or retaining the off-diagonal terms of the metric. The scaling is actually exact when the off-diagonal terms are included and valid to a good approximation when $Q_{\max} \gg 2$ in the other case.

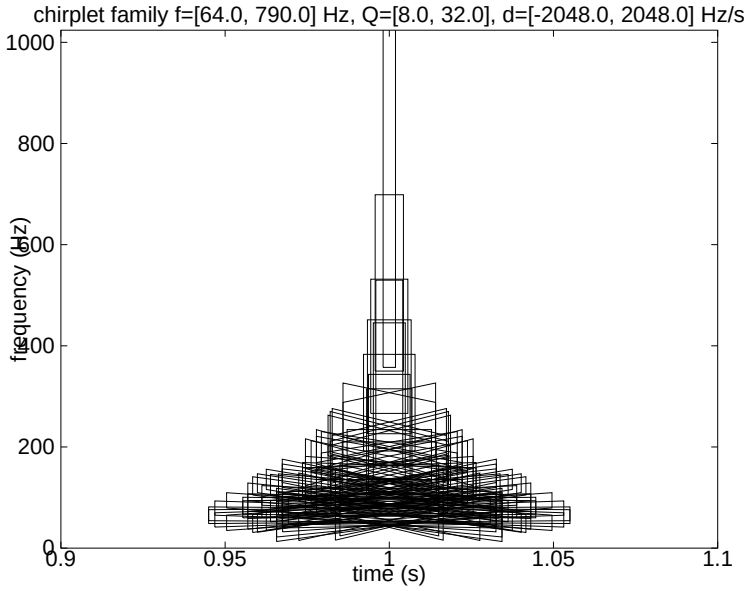

Figure 2. Example of a chirplet family resulting from the template placement procedure presented in Sec. 3. In this graph, each box represents the time-frequency tile associated with a chirplet. The oblique boxes are associated to non-zero values of the chirping rate d. The slope of the upper and lower edges equals d.

Chirplets with frequency exceeding this limits are aliased and have to be discarded. Fig. 3 also show the number of non-aliased chirplets. This number is about a factor of 10 larger than the number of sine-Gaussians required to cover the entire parameter space.

Two comments can be made at this point: the larger number of templates indicate that with chirplets, we define and explore a much larger signal space than with sine-Gaussians (we investigate this question further in Sec. 5). As the computing cost scales approximately linearly with the number of templates, analyzing the data with chirplets requires with a ten-fold increase in computing resources (a factor that will be rapidly absorbed by the exponential growth of computing power).

4. From "standard" to "chirpletized" Omega

In this session we discuss other aspects of the analysis pipeline, in addition to the implementation of the chirplet template bank.

4.1. Filtering

The modulus of $\Psi(\cdot)$ in Eq. (3) is a Gaussian function as in the sine-Gaussian case. This allows the use of the same filtering scheme as in the standard Omega pipeline to generate the chirplet transform. The Omega scheme [3] operates in the frequency domain following Eq. (2). It consists in multiplying the Fourier transform of the data, computed with the FFT algorithm, with that of the templates and take the inverse Fourier transform of the product. Omega uses a bi-square frequency window that approximates the Gaussian shape. The compact support of the bi-square window prevents aliasing.

This scheme can be applied to the chirplet case with two differences. First, the template Ψ is now complex, thus we need to multiply the data spectrum both in modulus and phase. Second, the template bandwidth now results from the quadratic sum $\Delta_f^2 = (\Delta_f^{\text{finite size}})^2 + (\Delta_f^{\text{chirp}})^2$ of two

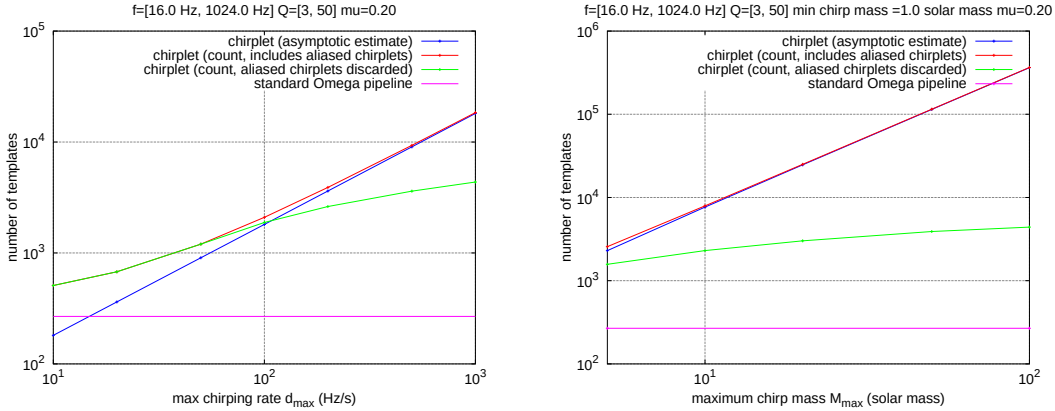

Figure 3. Size of the chirplet template bank in two cases: (*left*) assuming chirp rate limits between $\pm d_{\max}$ for any frequencies; (*right*) assuming frequency dependent limits consistent with the Newtonian model of the inspiralling binary chirp: $CM_{\min}^{5/3} f^{11/3} \lesssim d \lesssim CM_{\max}^{5/3} f^{11/3}$. The results are compared to the size of the sine-Gaussian template bank used by standard Omega. See text for a detailed discussion. All template banks are generated using the same maximum mismatch $\mu_{\max} = 0.2$.

components, one due to the finite size of the chirplet $\Delta_f^{\text{finite size}} = 1/\Delta_t$ and the other due to its sweeping frequency $\Delta_f^{\text{chirp}} = d\Delta_t$, where Δ_t is the chirplet duration (defined above). According to [3], the width of the bi-square window should be set to the chirplet frequency bandwidth Δ_f rescaled by a factor of $\sqrt{11}$.

4.2. Pre- and post-processing

In this paper we focus on a single-detector network, where most of the pre- and post-processing can be adopted from the standard Omega pipeline. Pre-processing consists of whitening the input data stream. Post-processing consists of selecting among the chirplets with partial time and frequency overlap to the one with maximum correlation with the data. Each chirplet is associated with a time-frequency tile, defined by $[t \pm \Delta_t/2, f \pm \Delta_f/2]$ where Δ_t and Δ_f are the chirplet duration and bandwidth, respectively. Two chirplets overlap if their time-frequency tiles overlap.

5. Performances of Chirpletized Omega

In this section we present a comparison between the standard version of the Omega pipeline, which uses sine-Gaussian wavelets, and its chirpletized version. We configure the pipelines with identical values for the parameters they have in common (frequency and Q range and maximum mismatch). We identify cases where we can expect advantages from analyzing the data with chirplets.

5.1. Analyzing chirplets with sine-Gaussians

The signal space associated with sine-Gaussians is contained in the larger space associated with chirplets. We estimate the signal-to-noise ratio (SNR) loss occurring when analyzing a chirplet by correlating this signal against a sine-Gaussian template bank. The chirplet parameters have been set to $Q = 50$, $f = 256$ Hz and $d = 2048$ Hz/s. Those parameters correspond to observable physical signals in the LIGO/Virgo frequency band (for instance, the selected chirping rate is approximately that of an inspiralling binary chirp with total mass $M \sim 3M_{\odot}$ – assuming equal

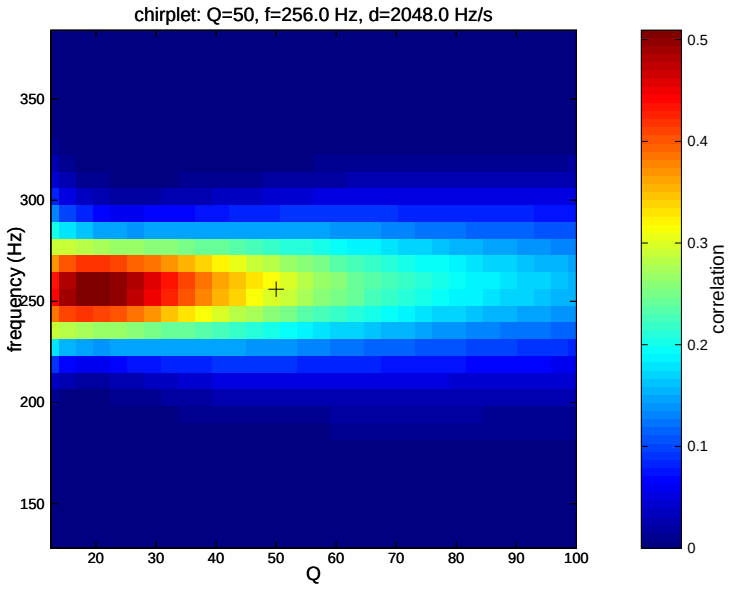

Figure 4. Correlation measurement between a single chirplet and a sine-Gaussian template bank. The parameters of the analyzed chirplet is indicated with a black cross in this diagram.

masses – at $f = 256$ Hz according to the Newtonian model). Fig. 4 presents the result of this analysis. Consistently to the metric estimate, the loss is $\sqrt{128}\pi f^2/(dQ^2) \sim 50\%$ in the present case. Note also that the maximum correlation is shifted to lower Q which may lead to a possible bias in the estimation of this parameter.

5.2. Analyzing inspiralling binary chirps with chirplets

One case study — As an illustration, we show here results from chirpletized Omega on simulated Gaussian noise, colored with the spectral characteristics of LIGO/Virgo noise with simulated gravitational wave signals. The signal we consider here results from the phenomenological approximation introduced in [2] of the coalescing binary black-hole chirp signals and includes the inspiral, merger and ringdown parts of the coalescence.

In Fig. 5, we compare the results from the standard and chirpletized Omega pipelines obtained for a black-hole binary chirp embedded in simulated Gaussian noise at large SNR. Chirplets with a positive slope are preferred to sine-Gaussian with constant frequency: the correlation of the most significative chirplet is, in this example, $\sim 45\%$ larger than the most significative sine-Gaussian. Work is currently in progress to understand how the background in chirpletized Omega is different from standard Omega. Preliminary studies in Gaussian noise suggest that the background rates are comparable, so that we can expect an increase of $\sim 30-40\%$ in distance reach by using chirplets.

Note that the chirplet slope provides indication of the frequency evolution of the observed signal and thus may be very useful in the *a posteriori* interpretation of an event.

Systematic study — We also performed a more systematic comparison over a population of inspiralling binaries. We considered a total of 5500 binaries with equal mass components. The total mass M is extracted from a flat distribution in the $4-100\,M_\odot$ range. The signal amplitudes are scaled so that the SNR is distributed over an interval ranging from ~ 10 to $\sim 10^3$.

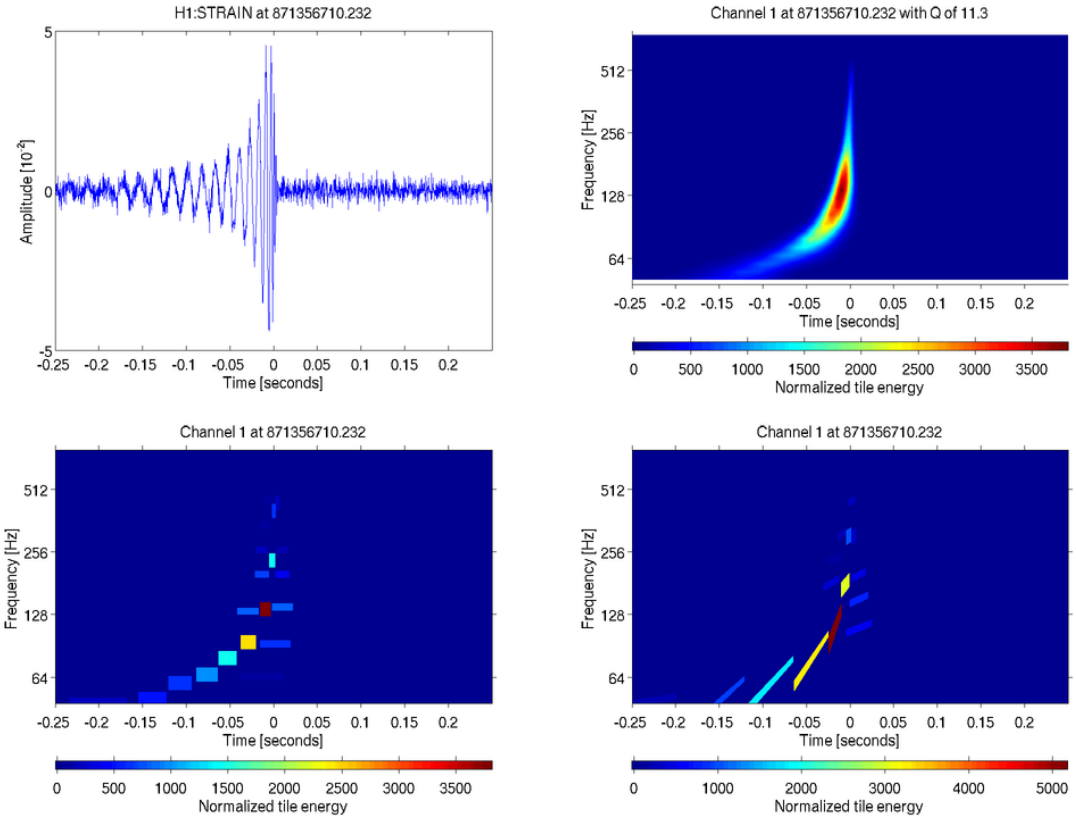

Figure 5. (*top/left*) Inspiralling black-hole binary (with masses $m_1 = 14M_\odot$, $m_2 = 16M_\odot$ and non-precessing spin parameters $\chi_1 = -0.68$ and $\chi_2 = -0.48$) signal in simulated Gaussian LIGO/Virgo-like noise. (*top/right*) Spectrogram (*bottom/left*) Significant time-frequency tiles for standard Omega (using sine-Gaussian wavelets only) (*bottom/right*) Significant time-frequency tiles for chirpletized Omega (using chirplets).

We obtain an estimate of the injected SNR from the amplitude of the most significant template. In the ideal case where signal and template are identical, the estimate equals the injected value. In Fig. 6, we show the relative difference of the SNR estimated by chirpletized Omega and standard Omega. Chirpletized Omega estimates a higher SNR across the mass range. However, there are two regimes: for the high-mass range $M \gtrsim 60M_\odot$, the SNR improvement is small ($\sim 5\%$) while it is more pronounced ($\sim 20\%$) for the low-mass range $M \lesssim 60M_\odot$. The improvement may go upto $\sim 40\%$ for $M \lesssim 20M_\odot$.

Generally speaking, the spectrum of the GW chirp is shifted toward low frequencies when the binary mass increases. The frequency associated with the innermost stable circular orbit (ISCO), which corresponds to the transition between inspiral and merger phase of the coalescence, is below 70 Hz for masses $M \gtrsim 60M_\odot$. In this condition, the chirp phase of the waveform with a spectral content at frequencies below ISCO is outside the detector sensitive band[4] and thus does not contribute significantly to the SNR. Sine-Gaussian waveform provides a good enough fit of the remaining few waveform cycles associated with the merger and ringdown parts of the coalescence. This explains the two regimes in Fig. 6.

[4] This statement is valid for the LIGO detector noise curve which was used for the systematic study. The mass cut-off is higher for the Virgo detector as its sensitive band extends to lower frequencies.

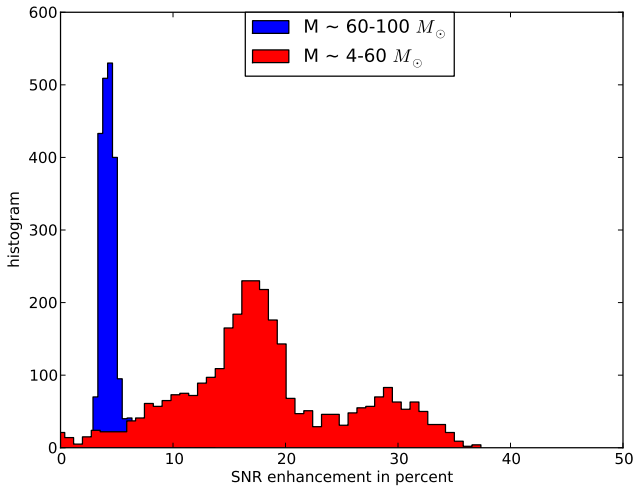

Figure 6. SNR enhancement from standard Omega to chirpletized Omega. The largest improvements about ~ 30 to 40% are mainly due to binaries in the low mass range $M < 20 M_\odot$.

6. Status and future plans

We introduced a new chirplet-based extension of the Omega pipeline. We show preliminary results using coalescing binary mergers waveforms. Versatility (robustness to signal model uncertainty) and algorithmic simplicity are two advantages of this methodology when compared to more standard approaches for the detection of such waveforms.

The single-detector network search code is ready and it can be downloaded [1] and used to produce chirpletized Omega scans similar to the one we show in Fig. 5.

We continue to study the response of the code to real noise and we aim at a complete, operating pipeline using chirplets as templates, and new clustering strategies tailored to these templates, as well as a multi-detector network strategy.

References

[1] `https://geco.phys.columbia.edu/omega/browser/branches/chirplet`.
[2] P. Ajith et al. 'Complete' gravitational waveforms for black-hole binaries with non-precessing spins, 2009. arXiv:0909.2867.
[3] S. K. Chatterji. The search for gravitational-wave bursts in data from the second LIGO science run. PhD thesis, MIT Dept. of Physics, 2005.
[4] B. J. Owen and B. S. Sathyaprakash. Matched filtering of gravitational waves from inspiraling compact binaries: Computational cost and template placement. Phys. Rev., D60:022002, 1999. gr-qc/9808076.

Acknowlegments

We are grateful to the LIGO Scientific Collaboration for the use of its algorithm library available at `https://www.lsc-group.phys.uwm.edu/daswg/projects/lalapps.html`. This work is supported in part by NSF grant PHY-0653550. M. Miele is supported by an ERASMUS fellowhip from the University of Sannio at Benevento (Italy).